Domain-wall dynamics, pinning, and nucleation in ultrathin epitaxial Fe films

R. P. Cowburn*
Cavendish Physics Laboratory, Madingley Road, Cambridge CB3 0HE, United Kingdom

J. Ferré
Laboratoire de Physique des Solides, associé au CNRS, Bâtiment 510, Université Paris-Sud, 91405 Orsay, France

S. J. Gray and J. A. C. Bland
Cavendish Physics Laboratory, Madingley Road, Cambridge CB3 0HE, United Kingdom
(Received 6 May 1998)

We have studied the dynamics of magnetic switching in in-plane magnetized ultrathin epitaxial Fe films by time-resolved magneto-optical magnetometry and microscopy. Experimental evidence has been found for two domain-wall pinning mechanisms: *macropins* and *micropins*. Macropins are extrinsic defects that are spatially distributed on the 10-μm length scale; micropins are intrinsic defects that are spatially distributed on a much shorter length scale. Once free from macropins, domain walls even in ultrathin films show line tension effects. We report a strong dependence on the magnetization direction of the relative importance of domain nucleation processes compared with domain-wall propagation processes. In-plane magnetized films do not readily nucleate reverse domains, whereas out-of-plane magnetized films of identical morphology do. This can be understood as being due to the different demagnetizing fields and domain-wall pinning energies.
[S0163-1829(98)01042-X]

I. INTRODUCTION

Ultrathin magnetic films have attracted much experimental and theoretical interest in recent years.[1] Under epitaxial growth conditions the magnetocrystalline anisotropies are very well defined across the entire crystal, and strong exchange coupling between atomic layers inhibits to first order any magnetization variations across the thickness of the film. The resulting magnet is therefore greatly simplified and so ultrathin epitaxial magnetic films are an excellent system for studying fundamental magnetic phenomena. From a technological point of view, thin and ultrathin magnetic films are promising candidates for use in high-density data storage and magnetoelectronic applications.[2]

An important area of study in thin-film magnetism is magnetic switching and domain structure. Magnetic switching is the process by which an applied field is used to change the direction of the magnetization in the film. Such magnetization changes are usually mediated by domain processes. Clearly this is of technological importance, because data storage, magnetic sensing, and magnetoelectronic signal processing all involve a change in spin direction. There is also strong fundamental interest in magnetic switching because important properties of the magnetic system such as coercivity, remanence, and susceptibility are all determined by the switching process. To date, several studies have been performed into the *statics* of magnetic switching,[3–5] but fewer have addressed the *dynamics*.[6] As will be demonstrated in this paper, switching dynamics can reveal important new information about fundamental interactions between the sample magnetism and morphology. A description of the temporal switching properties is also required for technological applications where signal bandwidth is at a premium.

The Fe/Ag(001) system is often used as a model ultrathin magnetic system for reasons that have been described more fully elsewhere.[7] A feature of this system that makes it particularly interesting is that by changing the Fe thickness only very slightly, the magnetization easy direction changes abruptly from being along the surface normal [Fe thicknesses less than about 5 ML to being in the plane (Fe thicknesses greater than about 5 ML)]. This change comes about through the so-called reorientation phase transition, which has recently been of great theoretical and experimental interest because of the possibility of thus realizing experimentally a two-dimensional Heisenberg magnet.[7,8] Furthermore, by using a sample with a wedge-shaped Fe thickness profile, two distinct magnetic systems can be studied with all other structural conditions remaining identical. We will make use of this important property of the Fe/Ag system to compare the dynamic spin reversal of the in-plane magnetized case with the out-of-plane magnetized case.

In this paper we will present the results of two experimental investigations into the dynamics of magnetic switching in in-plane magnetized ultrathin ($\sim$10 ML) epitaxial Fe/Ag(001) films. The first will use time-resolved magnetooptical magnetometry to observe magnetic relaxation (aftereffect) on the seconds time scale. The second will use time-resolved magnetooptical microscopy with pulsed magnetic fields to observe domain-wall (DW) motion on the nanosecond time scale. We will use these observations first to demonstrate the existence of two types of DW pinning defects present in the in-plane magnetized film and to show their consequences for the spin reversal dynamics. Second, we will make a comparison of the spin-reversal dynamics of an identical system when magnetized out of plane and when magnetized in plane. We will thus show a strong dependence on the relative importance of domain nucleation and DW propagation processes on the magnetization direction.

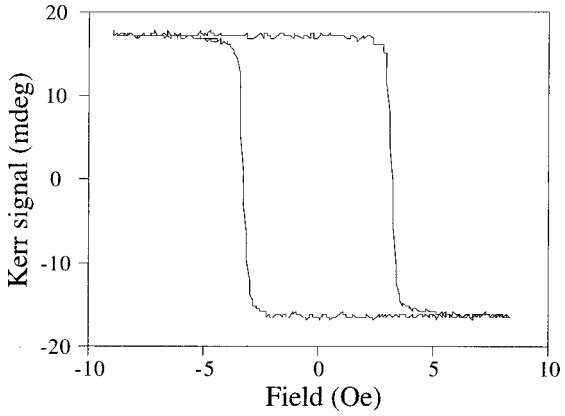

FIG. 1. A hysteresis loop measured by longitudinal MOKE under identical experimental conditions to those used for the relaxation measurements of Fig. 2.

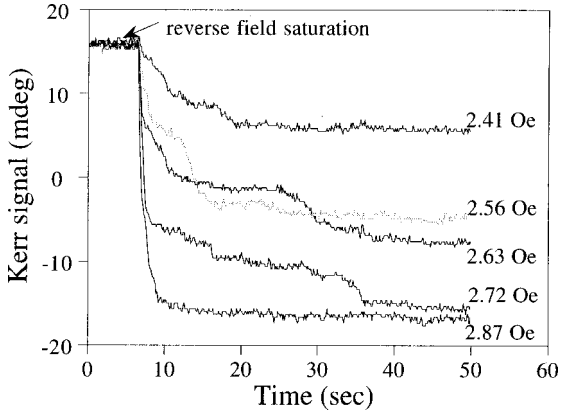

FIG. 2. Magnetic relaxation results. The applied field was rapidly switched at $t=7$ s from a large negative value to the value shown on the right-hand side of each trace. The graph shows the ensuing variation in Kerr signal as a function of time. The 2.56-Oe trace is shown in a different shade to distinguish it from the 2.63-Oe trace.

II. EXPERIMENT

A. Magnetic relaxation: Dynamics on the seconds time scale

Magnetic relaxation (also shown as magnetic aftereffect) is the phenomenon in which a change in the magnetic state of a system is delayed with respect to changes in an applied magnetic field.[9] A classic magnetic relaxation experiment is to saturate the sample with a large negative applied field, and then suddenly to switch the field to a value close to but still less than the positive coercive field. The magnetic state of the sample is then recorded as a function of time. At finite temperature, any subsequent magnetic changes are usually due to thermal activation. In cases where spin reversal proceeds via DW propagation, magnetic relaxation probes the ability of thermal activation to depin a DW and thus yields important information about the nature and distribution of the pinning sites. Where spin reversal is nucleation dominated, magnetic relaxation probes the probability of a nucleation event. Magnetic relaxation also has important technological implications, for it defines a time scale over which a ferromagnetic data storage system (e.g., recording media) will lose its memory.

We have measured magnetic relaxation using magnetooptics in an ultrathin Fe layer. All measurements reported in this section are for the case of the magnetization lying *in plane*. The sample consisted of a GaAs (001) substrate plus a 10-ML seed layer of Fe on which were grown $\sim$200 ML of Ag(001). The Fe layer of interest to this study was grown next with a wedge-shaped thickness profile allowing Fe thicknesses in the range 0–13 ML to be accessed. A further 10 ML of Ag were then deposited, followed by a 5-ML Cr protection cap. All depositions were performed in ultrahigh vacuum using molecular-beam epitaxy. Full details of the growth and structural and magnetic characterization have already been published.[3,7] A magnetooptical Kerr effect (MOKE) magnetometer using the longitudinal Kerr effect[10] with polarization modulation and operating at room temperature was used to probe the sample magnetization. The magnetometer laser beam was focused to a spot of diameter approximately 100 μm and so was sensitive to the component of magnetization aligned with an applied field averaged across this area. The sample was oriented such that the field was applied along the in-plane [100] direction of the ultrathin Fe layer, which is a magnetocrystalline easy axis. Our samples exhibit in addition to the usual bulk cubic anisotropy a very weak in-plane uniaxial anisotropy,[3] for which [100] was also an easy axis.

Figure 1 shows a hysteresis (M-H) loop measured by the magnetooptical magnetometer in order to determine the coercive field. The laser beam was focused onto a part of the wedge-shaped sample where the Fe thickness was 10 ± 1 ML and so the magnetization easy direction was in plane. The applied-field sweep rate was 8 Oe s^{-1}. A relaxation experiment was then performed in which a -6.3-Oe reverse saturating field was applied, which was then abruptly increased to a value H slightly smaller than the positive coercive field. The output from the magnetometer was recorded as a function of time for 43 s after the field switch. The experiment was then repeated for different H.

Figure 2 shows the results. The fact that the Kerr signal (and hence the average magnetization within the area of the focused laser spot) changes over time after the field switch shows that magnetic relaxation does indeed occur for these in-plane magnetized ultrathin samples. Strikingly, however, relaxation proceeds by a series of discrete jumps and not by the smooth evolution reported for out-of-plane magnetized systems.[11,12] Qualitatively similar results were produced at other points on the sample of similar Fe thickness and in other identical samples. Interestingly, our *same samples* produced smooth concave relaxation curves for Fe thicknesses sufficiently small that surface anisotropy forced the magnetization out of plane.[7]

The jumps in the Kerr signal during relaxation are $\sim$10% of the full signal range. It is already known from a previous nondynamic study[3] that magnetic switching proceeds by the sweeping of a few 180° DW's. Each relaxation jump therefore corresponds to a DW moving by $\sim$10 μm (100 μm beam diameter $\times$10%). We can thus postulate the existence of DW pinning sites that are spatially distributed on the 10-μm length scale. We shall discuss this further in Sec. III A.

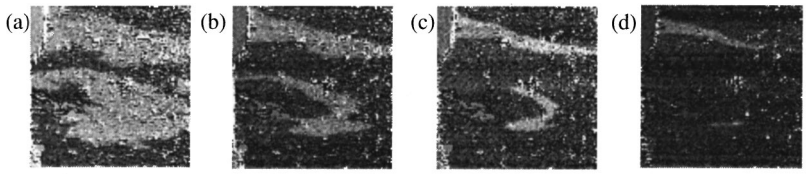

FIG. 3. (a) A domain structure created by slowly ramping a field up to the coercive field and then back to zero. Ten 16-ns pulses of 6 Oe amplitude were then applied for each of images (b)–(d). The original domain is white and the new domain is black, which correspond respectively to magnetization vectors pointing to the left and right of the image (or right and left; the absolute sign is unknown). Each image is 500×500 μm.

B. Pulsed magnetic-field microscopy: Dynamics on the nanosecond time scale

We have added a high-speed pulsed magnetic-field facility to a scanning Kerr microscope.[13] We can create in-plane top-hat field pulses directed along the sample [100] direction of up to 6 Oe amplitude and 2–18 ns width and with a subnanosecond rise time. These are generated by discharging a coaxial line charged to not more than 500 V through a microstrip into a 50-Ω load. A mercury-wetted reed relay is used as the switching element, the pulse width being determined by the length of the coaxial line.[14] The sample is glued onto the microstrip and so experiences the H field of the TEM wave that passes along the microstrip.

All of the results reported in this section were taken from the same sample as described in the previous section and at the same thickness (10 ± 1 ML). All of the DW's that will be observed are of the 180° Néel type, separating in-plane [100]- and [100]-oriented domains. We shall report the results of five different studies. In each case, a magnetic contrast image is taken by the microscope (a process that takes 4 min). Field pulses are then applied, and another image subsequently taken. The differences between the two images are assumed to be due to DW motion during the field pulse. Temporal information on the nanosecond time scale can thus be attained even though the microscope itself operates on a much slower time scale. As expected, no change in domain structure was observed after applying field pulses of amplitude less than the coercive field. This technique has also been used by Kirilyuk *et al.*[15]

Figure 3(a) shows a domain structure created by ramping a [100]-oriented magnetic field slowly from zero up to a value close to the coercivity and then back to zero. The sample was initially saturated in the [100] direction. [100] is defined as pointing to the right in the images. The low signal-to-noise ratio of the images is due to the small Kerr signal that comes from an ultrathin film (~15-mdeg Kerr rotation in this case) and the relatively wide signal passband (0–40 Hz) needed in the optical detection in order to acquire enough image pixels in a reasonable time. The majority of the permanent spots visible in all of the images are dust particles that greatly depolarize the reflected light. One sees that the DW's are rough and irregular, although not labyrinthine, with fluctuations on a length scale of approximately 10 μm. Figures 3(b)–3(d) show the result of then applying short field pulses. The black domain starts to grow and in doing so its walls become smoother and more regular.

In the second study, a DW was created in the same way as in the first study and then straightened by a few short pulses. Figure 4(a) shows the resulting wall. The DW was then propagated in 80-ns steps as shown in Figs. 4(b)–4(f). The difference images were obtained by numerically subtracting two consecutive images and so show how much the DW has moved in each step. One sees that most of the wall moves roughly the same distance each step. There are certain portions of the wall, however, that move less than other parts during a given step, e.g., right of center between Figs. 4(b) and 4(c), presumably due to some extraordinary pinning. When this happens, the rest of the wall moves on leaving the pinned part behind. The wall is therefore deformed and a ripple is introduced as seen clearly in images (b) and (f). The DW has an energy per unit length and so the deformation leads to an increase in energy, which in turn leads to tension within the wall. When the tension becomes too great, the pinned part is unpinned. Further propagation then tightens up the sag in the wall, so that even though image (c) shows a pinned portion that has been left behind, by image (d) the wall is completely straight again.

The third study concerns domain nucleation. It is a feature of magnetic films of high structural quality that magnetic switching proceeds by domain-wall sweeping.[12] A small number of nucleation events create the reverse domains that then grow by wall sweeping to cover the entire film. It is

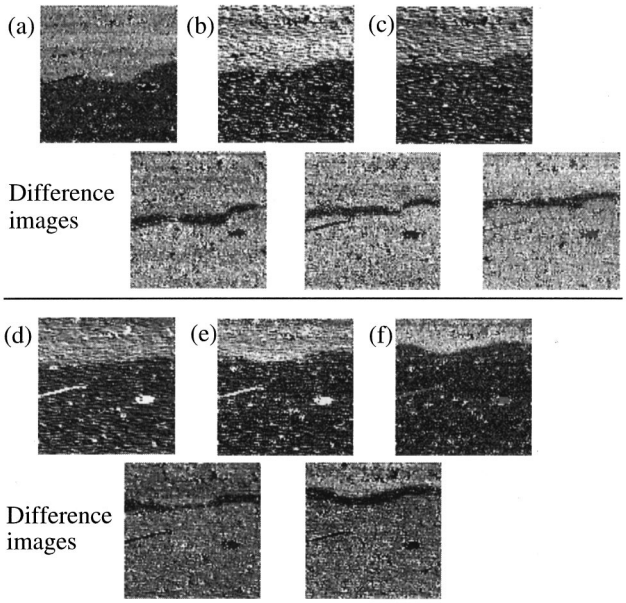

FIG. 4. A straight DW propagating under the action of short field pulses. Five 16-ns pulses of 6 Oe amplitude were applied between each of the images. The images without ( )'s show the difference between the two adjacent images. Each image is 200×200 μm.

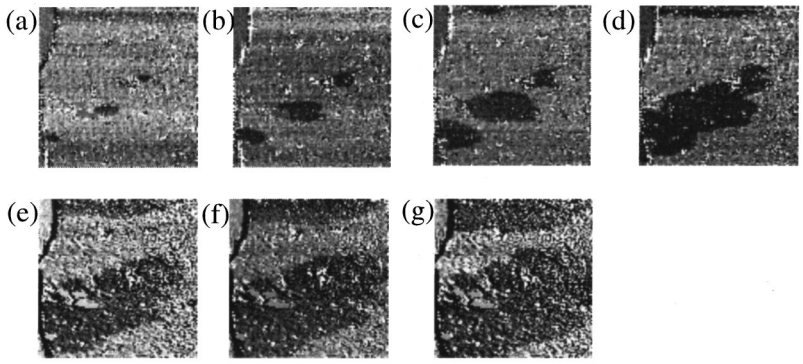

FIG. 5. The nucleation of new domains by field pulses. (a) was obtained by applying ten 16-ns pulses of 6 Oe amplitude to the sample just after saturation. The newly nucleated domains are then grown in (b)–(g) by 10 more pulses before each image. Each image is 500 $\times$500 μm.

therefore most unusual to observe the nucleation event directly in such films since they occur in a tiny fraction of the total surface area. Pulsed fields, however, allow nucleation to be studied directly. If a large pulsed field is applied, a nucleation event (which becomes more probable in higher fields) can occur before a DW from another part of the sample has had time to travel across the sample.[15] Figure 5 shows how starting from a single domain film it is possible to nucleate new domains by short field pulses, oriented as previously along the [100] direction. Figure 5(a) shows the nucleation centers. Further pulses cause these small domains to grow [(b) and (c)] until they begin to coalesce [image (d)]. Upon coalescence, the DW's straighten [image (e)] in the same way as described in the first study of this part and then begin to propagate in a straight line [(f) and (g)]. The fact that there are only three nucleation events in a 500$\times$500 μm area even though a field of twice the coercive field was being applied shows that the nucleation field of these films when magnetized in plane is very high relative to the DW propagation field. It is striking that nucleation should become so much more favorable when the same samples are magnetized out of plane.[7]

Figure 6 shows another example of pulsed field-induced nucleation. The microscope field of view was moved slightly to observe a different part of the sample (although of the same Fe thickness). The fact that the initially nucleated domains are so much more elongated than those of Fig. 5 and all lie in a straight line suggests that a tiny surface scratch is acting as a source of nucleation centers. The nucleated domains very quickly join up and then propagate across the surface.

For the fourth study, a domain was nucleated by applying pulses to a single domain film and then enlarged by a few further field pulses [Fig. 7(a)]. A high-resolution image was taken of the resulting domain [image (b)]. It can be seen that one of the domain vertices is pinned by a large surface defect located towards the lower left in both image (b) and the optical micrograph of (c). This observation agrees with that of the second study of this section that macroscopic surface defects can pin DW's.

In the fifth study, a DW was created by pulse induced nucleation of two small domains [Fig. 8(a)]. If one examines Figs. 8(a) and 8(b) carefully, it is possible to see the defect that acted as the nucleation center for the left-hand domain. These two domains were then grown by further pulses until they coalesced to form a large, straight-edged domain [image (b)]. The distance moved by two fixed points on one of these walls [indicated P and Q in image (b)] normal to the length of the wall was then measured at subsequent times in order to form a distance-time graph for the DW motion. This is shown in Fig. 9. One sees that the points form two good straight lines, showing that the portion of the wall marked P was propagating with a uniform velocity of $\pm 349 \pm 10$ ms^{-1} and that the portion marked Q was propagating uniformly at 303 ± 10 ms^{-1}. The fact that P is moving faster than Q explains why the normal to the DW appears to rotate between images (b) and (e) of Fig. 8. This velocity differential can be understood in similar terms to the straightening of the wall after depinning from a pinning site (Fig. 4). A wall that does not follow the magnetic easy axis has a higher energy than one that does because of magnetic charging. This is directly analogous to elastic beam bending, except that elastic potential energy is replaced by magnetostatic energy. A virtual work argument shows that the bent DW experiences a bending motion that increases the driving pressure on the parts that deviate from the easy axis. These therefore move faster than the parts that are aligned with the easy axis, until the bend is eliminated.

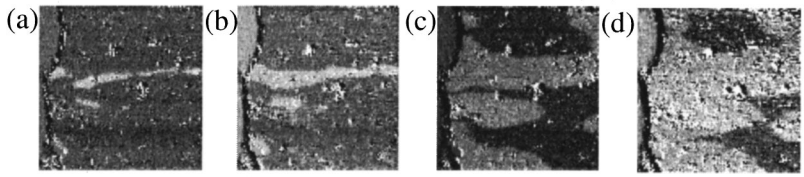

FIG. 6. A further example of nucleation by field pulses. (a) was obtained by applying two 18.5-ns pulses of amplitude 6 Oe to the sample just after saturation. (b)–(d) correspond to times 37, 180, and 277 ns later. Each image is 500$\times$500 μm.

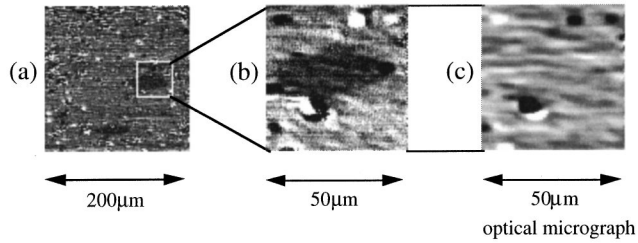

FIG. 7. A high-resolution view of pinning. The domain in (a) was nucleated and grown by four 18.5-ns pulses of 6 Oe amplitude. (b) shows the domain in high resolution. A surface defect can be seen in the optical micrograph to be holding one corner of the domain.

III. DISCUSSION

A. Domain-wall pinning: Evidence for micropins and macropins

The results from our magnetic relaxation experiment for the in-plane magnetized case reported DW's jumping in steps of approximately 10 μm. We were thus able to postulate the existence of domain-wall pinning sites spatially distributed on the 10-μm length scale. Atomic terraces have already been shown to be a potential source of DW pinning sites in ultrathin films.[16–18] However, the pinning sites detected in this relaxation experiment are distributed on a very much longer length scale than the mean atomic terrace length ($\sim$70 Å). We will therefore name these long length scale pinning sites *macropins.* The time-resolved images of the second part of this paper have confirmed the existence of such pinning sites. The scratch of Fig. 4(a) and the surface damage of Fig. 7(b) show that *extrinsic* defects are certainly able to act as macropins. In addition, Figs. 4(c) and 4(e) both show the DW being snagged by some invisible defect. The samples had not been subjected to rough handling, showing the sensitivity of the domain structure to very small imperfections. The dust particles visible in the microscope images are not considered to be sources of pinning defects because the relaxation behavior reported in part (a) was the same immediately after the sample was removed from the growth chamber as compared with that measured several months later.

The nanosecond time scale dynamic results cannot, however, be explained purely by the presence of macropins. The results of the fifth study of part (b) can only be explained by assuming the presence of a second type of pinning site. When the field pulse ends, the DW will come to rest at the nearest set of pinning sites, where it will later be imaged by the scanning microscope. The fact that we are able to construct a good distance-time graph in Fig. 9 with very little scatter on the points shows that these pinning sites must be distributed on a length scale that is much *shorter* than the distance between measurements ($\sim$10 μm). We therefore give the name of *micropins* to these pinning sites. Thus, in Fig. 4 it is the macropins that introduce the kinks into the DW at its propagates, but the micropins that hold it at the end of each field pulse. Compare the left-hand side of the wall in Fig. 4(a), which is held by a macropin (a short surface scratch) and is therefore characteristically roughened to the length scale of the macropins, with Fig. 4(d) where only micropins are acting, and so the wall is straight.

This also allows us to understand the smoothing of the DW by field pulses shown in Fig. 3. Figure 3(a) was taken using the so-called quasistatic imaging mode, where an applied field is slowly ramped up to a value close to the coercivity and then returned to zero. The resulting domain structure gives the distribution of pinning sites that were active at the maximum field value obtained. Now it is reasonable to assume that the pinning strengths of extrinsic macropins will be broadly distributed. Equally, although we cannot say anything *a priori* abut the distribution of the micropins, we can say that because of their much smaller spacing the DW will tend to average across many micropins simultaneously.[19] The depinning of a DW from a given micropin is therefore not an isolated event, but has partial coherence with neighboring micropins. This will narrow the distribution of the overall pinning strength experienced by the DW. Thus, we can suppose that the macropins will have the broader distribution, and as a result are more likely to be the active pinning sites at the maximum applied field. In short, the domain structure created by the quasistatic imaging mode will be dominated by macropins. This explains the rough nature of the wall in Fig. 3(a). Subsequent field pulses then free the wall from the macropins, and repin it at the end of the pulse at the nearest pinning site, which is most likely to be a micropin. Thus, the pulses change the dominant pinning type from macropin to micropin, and as a result the wall changes from rough (reflecting the length scale of the distribution of macropins) to smooth (reflecting the length scale of the distribution of micropins).

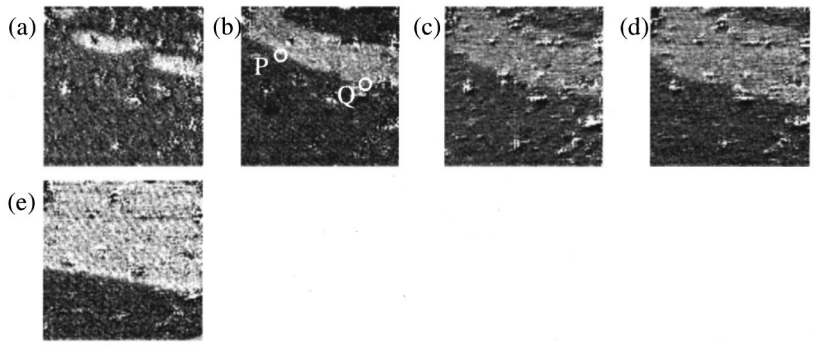

FIG. 8. Determination of DW propagation speed. (a) shows two domains that were nucleated and grown by applying two 18.5-ns pulses of 6-Oe amplitude. Two further pulses were then applied before each of (b)–(d). Four pulses were applied between (d) and (e). Each image is 200$\times$200 μm.

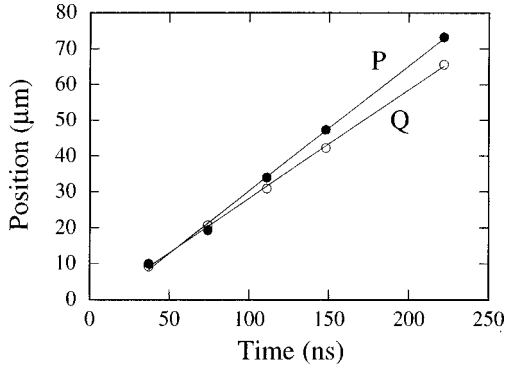

FIG. 9. Distance time graphs measured from the points *P* and *Q* of the propagating DW of Fig. 8.

A question that has received some attention recently is whether DW's in in-plane magnetized ultrathin films should be ''rough'' or ''smooth.'' Theoretical work has indicated that in the two-dimensional limit, the increase in entropy of a rough wall dominates over the increased magnetostatic energy, and so at finite temperature free energy is minimized by a roughening of the wall.[20,21] Experimental observations of rough DW's in films of a few ML's (Refs. 22–24) and of smooth DW's in thicker films[4] appear to confirm these predictions. However, there is also strong evidence that domain structure in real films is governed predominantly by pinning defects and not by entropy.[24] The results reported in this paper highlight the need for care in interpreting DW roughness in ultrathin films. Even though our samples are of high structural quality, the DW roughness is still determined by extrinsic and intrinsic defects. It is not surprising that domain structure in ultrathin films should be so very sensitive to defects given that a single atomic step corresponds to a 10% change in thickness and hence DW energy. Of particular significance is our finding that the quasistatic imaging method selects a very particular domain structure (i.e., one determined by extrinsic macropins).

B. Switching mechanisms and the magnetization direction

One of the striking features of our results is the observation that domain nucleation processes are far more prevalent when a sample is magnetized out of plane[7] than when the identical sample is magnetized in plane. There are two aspects to explaining this qualitatively.

First, the difference in anisotropy fields between the out-of-plane and in-plane magnetized cases acts to make the DW propagation field much greater for out-of-plane magnetized films than in plane. The anisotropy field determines the DW width and line energy and hence its interaction with defects. The anisotropy field in ultrathin out-of-plane magnetized films is generally dominated by the strong surface anisotropy term, which can be several kOe (except very close to the reorientation phase transition point where it is compensated by shape anisotropy). The anisotropy field in in-plane magnetized films is on the other hand dominated by bulk magnetocrystalline anisotropy that is typically only a few hundred Oe for ultrathin bcc epitaxial Fe.[25] Hence, the Bloch DW's appearing in out-of-plane magnetized films will be much narrower and much more energetically costly per unit length than the Néel walls of the in-plane magnetized film and so will be more strongly pinned by defects. This is in agreement with the experimental observation of our previous study[7] that found low-temperature (2 K) coercivities of ~ 40 Oe for in-plane magnetized ultrathin Fe films and ~ 500 Oe for the same samples when magnetized out of plane.

Second, the demagnetizing field, which is $4\pi M_s$ for out-of-plane magnetized films but which for in-plane magnetized ultrathin films tends to zero, acts to reduce the domain nucleation field for out-of-plane magnetized films with respect to the in-plane case. One can see this by writing the energy of an out-of-plane reverse domain of radius r as

$$U_{\perp} = 4\sqrt{AK_u}2\pi rt - 2\pi M_s^2 \pi r^2 t, \tag{1}$$

where A is the exchange stiffness, K_u is the total out-of-plane uniaxial anisotropy (i.e., surface + shape), M_s is the saturation magnetization, and t is the film thickness. For the case of an in-plane magnetized film, the corresponding energy would be

$$U_{\parallel} = 2\sqrt{AK_1}2\pi rt, \tag{2}$$

where K_1 is the cubic anisotropy constant. The Zeeman energy due to the applied field has been ignored because it contributes the same to the two cases. Domain nucleation is easier for the out-of-plane magnetized case than for the in-plane case (i.e., $U_{\perp} < U_{\parallel}$) for initial nucleation radii that satisfy

$$r > \frac{2\sqrt{A}(2\sqrt{K_u} - \sqrt{K_1})}{M_s^2 \pi}. \tag{3}$$

Substituting typical values of $A = 10^{-6}$ ergs cm^{-1}, $K_u = 5 \times 10^6$ ergs cm^{-3}, $K_1 = 10^5$ ergs cm^{-3}, and $M_s = 1700$ emu cm^{-3} into Eq. (3) gives $U_{\perp} < U_{\parallel}$ for $r > 9$ nm. Given that this is less than a typical DW width (~ 20 nm), this condition will be satisfied for all real nucleation events.

These two effects combine the make in-plane magnetized reversals propagation dominated and out-of-plane reversals nucleation dominated. We can thus explain our observation that when the film is magnetized out-of-plane magnetic relaxation proceeds by the nucleation of a large number of small domains, leading to a smooth, concave relaxation curve and when the film is magnetized in-plane relaxation proceeds by the sweeping of a small number of macropinned 180° DW's, leading to relaxation curves with abrupt jumps.

IV. CONCLUSION

We have studied in detail the dynamics of magnetic switching in an in-plane magnetized ultrathin film. Direct experimental evidence has been found for two DW pinning mechanisms: *macropins* and *micropins*. Macropins are physical defects that are spatially distributed on the 10-μm length scale and that largely determine the domain structure observed by the quasistatic imaging method. Surface scratches and other extrinsic defects have been shown to have macropinning ability. Micropins are physical defects that are spatially distributed on a length scale much shorter

than 10 μm; atomic step edges may be responsible for these. Once free from macropins, DW's even in ultrathin films show line tension effects.

We report that the ability of a film to nucleate reverse domains depends not only on its morphology, but also on the magnetization direction. The same sample that when magnetized in plane exhibited a great reluctance to nucleate reverse domains, even under the action of ''large'' applied fields (large relative to the coercive field), was able to nucleate domains very easily when magnetized out of plane. This observation can be understood as being due to the difference in demagnetizing fields between the in-plane and out-of-plane magnetized cases.

ACKNOWLEDGMENTS

This work was supported by the UK EPSRC, the DRA (UK), and EC Human Capital Mobility Network contract ''Novel magnetic films.'' R.P.C. also received additional support from the EC Human Capital Mobility Network and St. John's College, Cambridge.

*Present address: Nanoscale Science Group, Engineering Department, Cambridge University, Trumpington Street, Cambridge CB2 1PZ, United Kingdom.

[1] *Ultrathin Magnetic Structures,* edited by J. A. C. Bland and B. Heinrich (Springer-Verlag, Berlin, 1994).

[2] Y. Miura, J. Magn. Magn. Mater. **134**, 209 (1994); J. Heremans, J. Phys. D **26**, 1149 (1993); M. Johnson, J. Magn. Magn. Mater. **156**, 321 (1996); H. How, T. M. Fang, and C. Vittoria, IEEE Trans. Microwave Theory Tech. **43**, 1620 (1995).

[3] R. P. Cowburn, S. J. Gray, J. Ferré, J. A. C. Bland, and J. Miltat, J. Appl. Phys. **78**, 7210 (1995); R. P. Cowburn, S. J. Gray, and J. A. C. Bland, Phys. Rev. Lett. **79**, 4018 (1997).

[4] E. Gu, J. A. C. Bland, C. Daboo, M. Gester, L. M. Brown, R. Ploessl, and J. N. Chapman, Phys. Rev. B **51**, 3596 (1995).

[5] J. L. Robins, R. J. Celotta, J. Unguris, D. T. Pierce, B. T. Jonker, and G. A. Prinz, Appl. Phys. Lett. **52**, 1918 (1988); J. M. Florczak and E. Dan Dahlberg, Phys. Rev. B **44**, 9338 (1991); J. Chen and J. L. Erskine, Phys. Rev. Lett. **68**, 1212 (1992); J. R. Childress, R. Kergoat, O. Durand, J.-M. George, P. Galtier, J. Miltat, and A. Schuhl, J. Magn. Magn. Mater. **130**, 13 (1994); R. Allenspach, *ibid.* **129**, 160 (1994); W. Weber, C. H. Bach, A. Bischof, D. Pescia, and R. Allenspach, Nature (London) **374**, 6525 (1995).

[6] M. J. Baird, J. A. C. Bland, E. Gu, A. J. R. Ives, F. O. Schumann, and H. P. Hughes, J. Appl. Phys. **74**, 5658 (1993).

[7] R. P. Cowburn, J. Ferré, J.-P. Jamet, S. J. Gray, and J. A. C. Bland, Phys. Rev. B **55**, 11 593 (1997).

[8] N. D. Mermin and H. Wagner, Phys. Rev. Lett. **17**, 1133 (1966); M. Bander and D. L. Mills, Phys. Rev. B **38**, 12 015 (1988); R. P. Erickson and D. L. Mills, *ibid.* **46**, 861 (1992); P. J. Jensen and K. H. Bennemann, *ibid.* **42**, 849 (1990); D. Pescia and V. L. Pokrovsky, Phys. Rev. Lett. **65**, 2599 (1990); Y. Yafet and E. M. Gyorgy, Phys. Rev. B **38**, 9145 (1988); D. P. Pappas, C. R. Brundle, and H. Hopster, *ibid.* **45**, 8169 (1992); Z. Q. Qiu, J. Pearson, and S. D. Bader, Phys. Rev. Lett. **70**, 1006 (1993); A. Berger and H. Hopster, *ibid.* **76**, 519 (1996); S. D. Bader, Dongqi Li, and Z. Q. Qiu, J. Appl. Phys. **76**, 6419 (1994).

[9] S. Chikasumi, *Physics of Magnetism* (Krieger, Malabar, 1978), Chap. 15.

[10] K. Sato, Jpn. J. Appl. Phys. **20**, 2403 (1981).

[11] M. Labrune, S. Andrieu, F. Rio, and P. Bernstein, J. Magn. Magn. Mater. **80**, 211 (1989); G. Bayreuther, P. Bruno, G. Lugert, and C. Turtur, Phys. Rev. B **40**, 7399 (1989).

[12] J. Pommier, P. Meyer, G. Pénissard, J. Ferré, P. Bruno, and D. Renard, Phys. Rev. Lett. **65**, 2054 (1990).

[13] P. Kasiraj, R. M. Shelby, J. S. Best, and D. E. Horne, IEEE Trans. Magn. **22**, 837 (1986); W. W. Clegg, N. A. E. Heyes, E. W. Hill, and C. D. Wright, J. Magn. Magn. Mater. **95**, 49 (1991); P. Büscher and L. Reimer, Scanning **15**, 123 (1993).

[14] J. M. Pettit, *Electronic Switching, Timing and Pulse Circuits* (McGraw-Hill, London, 1958).

[15] A. Kirilyuk, J. Ferré, J. Pommier, and D. Renard, J. Magn. Magn. Mater. **121**, 536 (1993).

[16] P. Bruno, G. Bayreuther, P. Beauvillain, C. Chappert, G. Lugert, D. Renard, J. P. Renard, and J. Seiden, J. Appl. Phys. **68**, 5759 (1990).

[17] D. Sander, R. Skomski, C. Schmidthals, A. Enders, and J. Kirschner, Phys. Rev. Lett. **77**, 2566 (1996).

[18] R. P. Cowburn and J. A. C. Bland (unpublished).

[19] S. Lemerle, J. Ferré, C. Chappert, V. Mathet, T. Giamarchi, and P. LeDoussal, Phys. Rev. Lett. **80**, 849 (1998).

[20] S. T. Chui, Phys. Rev. B **51**, 250 (1995).

[21] S. J. Robinson, J. Castro, and G. A. Gehring, J. Magn. Magn. Mater. **156**, 133 (1996).

[22] H. P. Oepen, J. Magn. Magn. Mater. **93**, 116 (1991).

[23] R. Schäfer, J. Magn. Magn. Mater. **148**, 226 (1995).

[24] A. Berger, U. Linke, and H. P. Oepen, Phys. Rev. Lett. **68**, 839 (1992).

[25] R. P. Cowburn, A. Ercole, S. J. Gray, and J. A. C. Bland, J. Appl. Phys. **81**, 6879 (1997).